A visually guided swim assay for mouse models of human retinal disease recapitulates the multi-luminance mobility test in humans

Salma Hassan[1,2], Ying Hsu[2], Sara K. Mayer[2,3], Jacintha Thomas[2*], Aishwarya Kothapalli[2#], Megan Helms[2 ^], Sheila A. Baker[4], Joseph G. Laird[4], Sajag Bhattarai[2], Arlene V. Drack[1,2,3,5]

Access this article online

Quick Response Code:

Website: www.saudijophthalmol.org

DOI: 10.4103/sjopt.sjopt_155_23

[1]Department of Anatomy and Cell Biology, Biomedical Science- Cell and Developmental Biology Graduate Program, [2]Department of Ophthalmology and Visual Sciences, IVR, [3]Interdisciplinary Genetics Program, [4]Department of Biochemistry, [5]Department of Pediatrics, University of Iowa, Iowa City, IA, USA

Address for correspondence:
Prof. Arlene V. Drack, Department of Ophthalmology and Visual Sciences, University of Iowa, 200 Hawkins Drive, Iowa City, Iowa 52242, USA.
E-mail: arlene-drack@uiowa.edu

Current address:
*Kirksville College of Osteopathic Medicine, A.T. Still University, Kirksville, MO, USA, #University of Iowa - Des Moines Internal Medicine Residency Program, Iowa Methodist Medical Center, Des Moines, IA, USA, ^Advocate Illinois Masonic Medical Center, Chicago, IL, USA

Submitted: 12-Jul-2023
Revised: 24-Jul-2023
Accepted: 26-Jul-2023
Published: 18-Nov-2023

Abstract:

PURPOSE: The purpose of this study was to develop a visually guided swim assay (VGSA) for measuring vision in mouse retinal disease models comparable to the multi-luminance mobility test (MLMT) utilized in human clinical trials.

METHODS: Three mouse retinal disease models were studied: Bardet–Biedl syndrome type 1 (*Bbs1*$^{M390R/M390R}$), $n = 5$; Bardet–Biedl syndrome type 10 (*Bbs10*$^{-/-}$), $n = 11$; and X linked retinoschisis (retinoschisin knockout; *Rs1*-KO), $n = 5$. Controls were normally-sighted mice, $n = 10$. Eyeless *Pax6*$^{Sey\text{-}Dey}$ mice, n = 4, were used to determine the performance of animals without vision in VGSA.

RESULTS: Eyeless *Pax6*$^{Sey\text{-}Dey}$ mice had a VGSA time-to-platform (TTP) 7X longer than normally-sighted controls ($P < 0.0001$). Controls demonstrated no difference in their TTP in both lighting conditions; the same was true for *Pax6*$^{Sey\text{-}Dey}$. At 4–6 M, *Rs1*-KO and *Bbs10*$^{-/-}$ had longer TTP in the dark than controls ($P = 0.0156$ and $P = 1.23 \times 10^{-8}$, respectively). At 9–11 M, both BBS models had longer TTP than controls in light and dark with times similar to *Pax6*$^{Sey\text{-}Dey}$ ($P < 0.0001$), demonstrating progressive vision loss in BBS models, but not in controls nor in *Rs1*-KO. At 1 M, *Bbs10*$^{-/-}$ ERG light-adapted (cone) amplitudes were nonrecordable, resulting in a floor effect. VGSA did not reach a floor until 9–11 M. ERG combined rod/cone b-wave amplitudes were nonrecordable in all three mutant groups at 9–11 M, but VGSA still showed differences in visual function. ERG values correlate non-linearly with VGSA, and VGSA measured the continual decline of vision.

CONCLUSION: ERG is no longer a useful endpoint once the nonrecordable level is reached. VGSA differentiates between different levels of vision, different ages, and different disease models even after ERG is nonrecordable, similar to the MLMT in humans.

Keywords:

Dark-adapted , electroretinogram, functional vision, light-adapted, retinal degeneration, visually guided swim assay

Introduction

Preclinical treatment studies in mouse models of human genetic retinal disorders have paved the way for the first FDA-approved subretinal gene replacement treatment and numerous clinical trials.[1,2] Electroretinogram (ERG) amplitudes are often used as a treatment endpoint to assess efficacy in murine studies because it is an objective measure of retinal cell activity.[3-5] However, in mice as in humans, the ERG becomes nonrecordable before all vision is lost,[6,7] making subtle treatment effects impossible to measure. Activity from a substantial number of functional photoreceptors is required for the electrical activity to be recordable on full-field ERGs.[8] However, it is possible that the rescue of small foci of photoreceptors by treatment can provide some measures of useful vision.[9] In addition, ERG is not a direct measure of functional vision.[10] Therefore, a functional measure of vision for

How to cite this article: Hassan S, Hsu Y, Mayer SK, Thomas J, Kothapalli A, Helms M, *et al*. A visually guided swim assay for mouse models of human retinal disease recapitulates the multi-luminance mobility test in humans. Saudi J Ophthalmol 2023;37:313-20.

rodents is needed to quantitatively assess vision loss over the disease course, as well as determine the efficacy of treatments. This would be analogous to the multi-luminance mobility test (MLMT), a functional vision test that measures the impact of varying levels of illumination on an individual's ability to navigate surroundings. The MLMT provides quantitative data on mobility performance and was chosen as an endpoint for the human clinical trials of gene therapy with voretigene neparvovec (now Luxturna®).[11,12]

Experimental methods to measure rodent vision exist, such as measurements of optokinetic nystagmus and optomotor response/reflex.[13,14] While these methods offer valuable insights into certain aspects of vision, they lack direct assessment of functional vision because they only measure the reflexive eye movements in response to visual stimuli and not the ability of mice to navigate using vision. The Morris water maze has been modified by several investigators to assess visually guided navigation.[15-19] Not all of these methods of testing have been validated fully with normally-sighted versus completely blind mice, nor have they been correlated with ERG.

In this study, we provide evidence that the visually guided swim assay (VGSA), modified from the Morris water maze,[15-19] can measure subtle differences and changes in functional vision throughout the disease course of mouse models with retinal degeneration. We compare models of two subtypes of Bardet–Biedl syndrome (BBS), an autosomal-recessive syndrome that includes rapid retinal degeneration leading to legal blindness[10,20-22] with a model of X-linked retinoschisis (XLRS), a disease-causing cystic macular degeneration in humans which is relatively stable for most of the lifespan.[23] To standardize the assay, we have included eyeless *Pax6*$^{Sey\text{-}Dey}$ mice, which completely lack vision due to anophthalmia.[24,25]

Methods

Animals

Experiments were conducted in accordance with guidelines established by the Institutional Animal Care and Use Committee and adhered to the Association for Research in Vision and Ophthalmology guidelines for animal use in vision research. Animals were housed in standard cages with *ad libitum* access to food and water and were maintained on a 12-h light-dark cycle. Mouse model *Bbs1*$^{M390R/M390R}$ was generated as described previously.[26,27] The *Bbs10* mouse model was previously described.[10] *Rs1*-KO mice were a gift from Paul Sieving, M.D., Ph.D.[28-30] *Pax6*$^{Sey\text{-}Dey}$ (stock #000391)[24,25] and wild-type control *SV129* mice were obtained from Jackson Laboratory, Bar Harbor, Maine.

Four groups of mice were assessed at age 4–6 months (M): These groups consisted of group 1: 11 *Bbs10*$^{-/-}$ mice, group 2: 5 *Rs1*-KO mice, group 3: 5 *Bbs1*$^{M390R/M390R}$ mice,[26] and group 4: 10 controls consisting of five heterozygous unaffected *Bbs1*$^{M390R/+}$mice, four heterozygous unaffected *Bbs10*$^{+/-}$ mice, and one wild-type *SV129* mouse. At 9–11 M, the mice were retested along with four *Pax6*$^{Sey\text{-}Dey}$ eyeless mice. The *Bbs1*$^{M390R/M390R}$ mouse data included here have been reported previously.[10]

Apparatus

The visually guided swim assay (VGSA) was developed using a plastic children's swimming pool (Splash Time, H20 model #1015, Gracious Living Corporation, Woodbridge, Ontario, Canada). The pool had a diameter measuring 36" at the bottom, 39" at the 4-inch water level, and 42" at the top. The platform positions were marked, as shown in Figure 1a and b. The mouse entry location was from the position nearest platform #1 [red X point in Figure 1a]. A 3" diameter PVC tube with rubber caps on both ends was used as a platform for the mice to climb on to end the trial. The platform was flipped in the water between trials to mitigate scent. A small flag was attached to the platform to increase its visibility. The pool was filled to 1 cm below the surface of the platform and maintained at a temperature of 22°C–23°C. If the mice could not find the platform in the allotted time during training, they were guided to the platform. Two sequential sets of experiments were performed, first light-adapted (LA) under normal room light measuring 13.35 cd/m^2 and then dark-adapted (DA) in dim red lighting measuring approximately 4.17×10^{-3} cd/m^2. The measurement of the dim red light was taken at the surface of the water. During dark trials, investigators utilized a night vision monocular (TKKOK M60), as needed to view the mice [Figure 1c]. The individual in the photograph granted permission for its use. The VGSA was developed based on modifications of the Morris Water Maze[15,31] and has been described briefly elsewhere.[10,32]

Training and testing

Before LA testing began, mice were trained to swim to the platform in LA conditions. LA training involved 4 days of swimming, 5 trials a day, each to a randomized platform location. On the first 2 training days, each mouse was allowed to swim for 30 s while searching for the platform, after which it was guided to the platform using a plastic tray until it climbed upon it. On the following 2 training days, the mice were allowed to swim for 45 s searching for the platform. After each training trial, the mouse was allowed to rest on the platform for 30 s after which the mouse was gently removed from the platform, dried, and placed back into its cage. After the 4 days of training, 4 days of testing were performed.[33,34] Both training and testing took place in the afternoon for consistency. Each mouse was held vertically by its tail, with its back legs on the side of the pool at the placement position, so its front legs just touched the water, facing forward. The mouse was gently placed into the water and a timer was started. If the mouse floated instead of swimming, finger snapping or tail squeezing was used to incite movement. Once the mouse acknowledged the platform by placing (at least) both front paws on it, the timer was stopped, and time was recorded. Each mouse was allowed to search for the platform for up to 60 s unassisted during testing, after which it was removed from the water to prevent fatigue, dried, and returned to the cage. After each trial, the platform was splashed with water to remove the scent. Once all the mice in the trial had

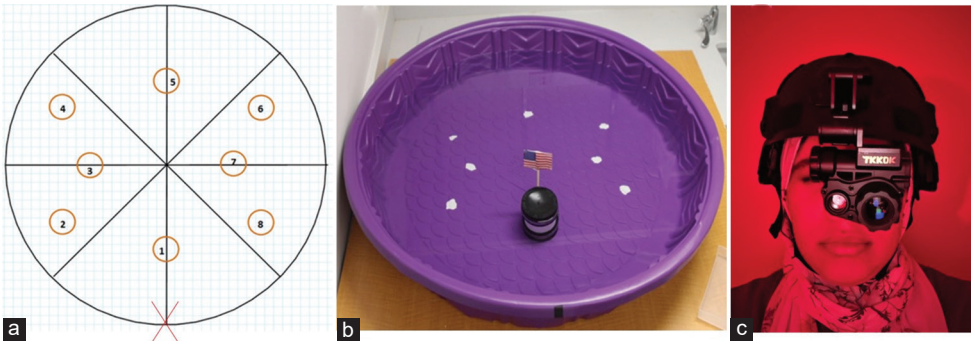

Figure 1: Visually guided swim assay setup. (a) Schematic of pool setup. Circles determine the possible platform positions. Image to scale. 1 square = 1 inch. The red X denotes the mouse entry location. (b) Photo of experimental assay setup. Measurements follow the schematic to the left. (c) A night vision monocular used by investigators to view the mice during dark-adapted conditions. The individual in the photograph granted permission for its use

swum to the same platform location, the platform was flipped in the water and moved to a new random location. Out of eight possible locations, five were chosen each day without repeating patterns from the previous day. Adjacent platforms were not chosen in sequence to prevent the potentially confounding effect of using memory to locate the platform.

DA training followed the LA testing and was therefore conducted for only 2 training days prior to 4 days of DA testing. Mice were kept in a dark room for 2 h before DA training. On the 1st day of DA training, each mouse was given 30 s to find the platform before being guided; on the 2nd day, the mouse was allowed to swim for 45 s before being guided. The mice were allowed to rest on the platform for 30 s after finding it. For DA testing, the mice were again DA for 2 h just as they were before DA training.

During the DA protocols, a night vision monocular was worn by the examiner who placed the mouse in the pool to enable mouse visualization [Figure 1c] while another investigator strictly controlled the stopwatch and recorded the TTP. Investigators were masked to the genotype of each mouse to eliminate bias.

The TTPs from every swim test for a given lighting condition were averaged for each mouse to get its average TTP. Only times recorded on the 4 testing days in each lighting condition were used as data. The number of times each mouse floated or had to be removed from the water at 60 s without attaining the platform was recorded. All data from a mouse were excluded if, during a test day, a mouse's mean TTP was >1 standard deviation from their genotype's median and the mouse floated more than three times per test episode. After trials each day, mice were left in their cages on a 36°C heating pad until dry. The pool was emptied, and the pool and platform were cleaned. Trials were videotaped using a Canon EOS 5D Mark II body with a Canon EF 28–105 mm f/3.5–4.5 USM lens (Canon, Tokyo, Japan) modified to be infrared only.

Electroretinogram protocol

A modified International Society for Clinical Electrophysiology of Vision protocol[35] was used as described in detail elsewhere.[10,32]

Statistical analysis

The statistical analysis was conducted using GraphPad PRISM 9.0 (GraphPad Software, Inc, San Diego, California, USA). One-way analysis of variance (ANOVA) was used to analyze the difference between experimental groups, and two-way ANOVA was used to analyze the difference between groups over time, followed by the multiple comparisons *post hoc* Tukey's test (nonparametric). The correlation between ERG data and TTP was assessed using RStudio version 4.2.2. Throughout the analyses, an alpha value of 0.05 was used as the significance threshold. The reported values in the results are presented as averages ± standard deviation.

Results

Comparative analysis of TTP between eyeless mice and normally-sighted control mice

Normally-sighted control mice and eyeless *Pax6*$^{Sey\text{-}Dey}$ mice were tested to determine how mice with proper eyesight versus no eyesight perform during the VGSA [Figure 2]. No eye formation was observed in *Pax6*$^{Sey\text{-}Dey}$ mice [Figure 2a-c]; these mice are otherwise physically and developmentally normal. When comparing the two groups at the age of 9–11 M, they were significantly different from each other in light (control: 3.330 ± 1.108 s; *Pax6*$^{Sey\text{-}Dey}$: 30.23 ± 6.49 s; $P = 5 \times 10^{-7}$, one-way ANOVA, *post hoc* Tukey's test) and in dark (control: 4.342 ± 0.828 s; *Pax6*$^{Sey\text{-}Dey}$: 30.09 ± 12.16 s; $P = 9 \times 10^{-7}$, one-way ANOVA, *post hoc* Tukey's test). Neither controls nor *Pax6*$^{Sey\text{-}Dey}$ exhibited any difference in TTP between light and dark performance [Figure 2d]. The TTPs of control and eyeless *Pax6*$^{Sey\text{-}Dey}$ mice serve as reference points for the performance of mice with normal vision, about 4 s, and mice without any vision, about 30 s.

Visually guided swim assay differentiates between different types of retinal degeneration

To determine whether this assay can detect differences in functional vision in mouse models with retinal disease, five groups of mice were tested in both light and dark conditions: *Bbs1*$^{M390R/M390R}$, *Bbs10*$^{-/-}$, *Rs1*-KO, *Pax6*$^{Sey\text{-}Dey}$, and normally-sighted controls. All mice except *Pax6*$^{Sey\text{-}Dey}$ were initially assessed between 4 and 6 M and then again between 9 and 11 M. *Pax6*$^{Sey\text{-}Dey}$ mice were only assessed at 9–11 M [Figure 2].

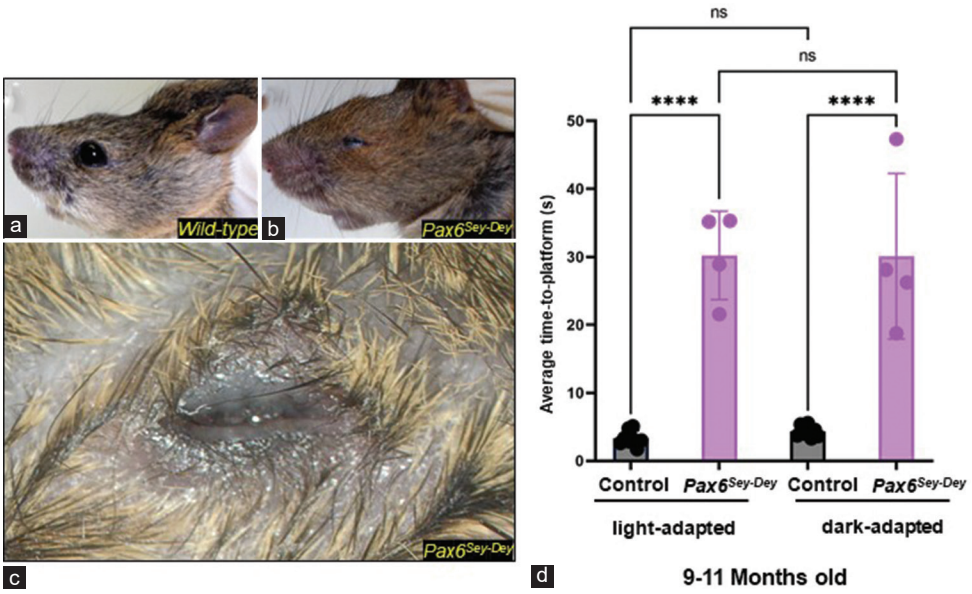

Figure 2: Comparison of *Pax6*$^{Sey\text{-}Dey}$ and control mice. (a) Wild-type mouse with normal eye development. (b) Photo of *Pax6*$^{Sey\text{-}Dey}$ mouse showing absent eye. (c) Close-up photo of anophthalmic *Pax6*$^{Sey\text{-}Dey}$ mouse; right and left ocular regions in mice selected for the study were the same. (d) Comparison of time-to-platform (TTP) at 9–11 M for control mice and *Pax6*$^{Sey\text{-}Dey}$ in both light and dark. Difference in TTP between genotypes at the same light level is significant. There was no difference in TTP between light and dark in mice of the same genotype. Control: Wild-type or heterozygous mice. s = seconds. **** = $P < 0.0001$. ns = not significant

The TTP for each mouse, a metric representing the time it takes for a mouse to locate the platform, was calculated by averaging the 20 different swim trials for that mouse in the light and the dark, respectively. There was no difference in the TTP for control mice as they aged in either the light (4–6 M: 5.069 ± 1.896 s; 9–11 M: 3.330 ± 1.108 s; $P = 0.725$) or the dark (4–6 M: 5.494 ± 1.675 s; 9–11 M: 4.342 ± 0.8218 s; $P = 0.929$), demonstrating that functional vision remains stable in control mice over time [Figure 3a and b].

At 4–6 M [Figure 3c and d], the average TTP for *Bbs1*$^{M390R/M390R}$ was not significantly different from the control in either light (*Bbs1*$^{M390R/M390R}$: 5.338 ± 2.969 s; $P = 0.490$) or dark (*Bbs1*$^{M390R/M390R}$: 10.77 ± 4.403 s; $P = 0.9964$). This indicates that even though *Bbs1*$^{M390R/M390R}$ mice already have photoreceptor cell loss and abnormal ERG at this age,[10] their functional vision has not been grossly impacted. Conversely, at 4–6 M, *Bbs10*$^{-/-}$ mice demonstrated significantly longer TTP than controls in both lighting conditions (*Bbs10*$^{-/-}$: 12.24 ± 6.86 s, $P = 0.0038$ in the light, and 26.24 ± 6.138 s while DA, $P = 1.23 \times 10^{-8}$). This agrees with prior reports, stating that the disease course progresses faster in BBS10 than in BBS1 in humans[36] and in mice.[10] At 4–6 M, *Rs1*-KO mice had a TTP of 3.154 ± 0.42 s in the light, which is not different than that of control mice ($P = 0.903$), and 14.99 ± 6.96 s in the dark, which is significantly longer than control mice ($P = 0.0156$, one-way ANOVA, *post hoc* Tukey's test) but shorter than that of the BBS model. These data indicate that VGSA provides quantitative metrics for functional vision in the light and in the dark and can differentiate between different retinal disorders.

At 9–11 M [Figure 3e and f] in both lighting conditions, the TTP for *Bbs1*$^{M390R/M390R}$ mice was significantly longer than that of the controls (*Bbs1*$^{M390R/M390R}$: 24.89 ± 6.60 s in the light, $P = 1.28 \times 10^{-7}$, and 24.34 ± 6.825 s in the dark, $P = 1.6219 \times 10^{-5}$, one-way ANOVA, *post hoc* Tukey's test), indicating that their vision had deteriorated. At 9–11 M, *Bbs10*$^{-/-}$ mice had longer TTP in the light than they had at 4–6 M (*Bbs10*$^{-/-}$: 30.66 ± 6.60 s, $P = 3 \times 10^{-12}$, in the light and 33.26 ± 6.69 s, $P = 7.43 \times 10^{-11}$, in the dark).

At 9–11 M, *Bbs1*$^{M390R/M390R}$ and *Bbs10*$^{-/-}$ mice were similar to each other and to the eyeless *Pax6*$^{Sey\text{-}Dey}$ mouse group. The *Rs1*-KO group had much better TTP compared to *Pax6*$^{Sey\text{-}Dey}$ and the BBS models, showing that the swim assay can detect different functional vision levels in mice with different retinal diseases.

Visually guided swim assay correlates with electroretinogram b-wave and is more sensitive than electroretinogram at distinguishing functional vision

To determine the correlation of functional vision with ERG, ERG was performed for each mouse at age 4-6 M and again at age 9–11 M [Figure 4], except in the eyeless *Pax6*$^{Sey\text{-}Dey}$ mice. The DA standard combined response (SCR) b-wave, elicited with a stimulus of 3.0 cd·s/m^2, was analyzed as a measure of rods and cones. The b-wave amplitudes of all affected retinal disease models, even at ages 4–6 M, were lower than those of control mice ($P < 0.0001$) [Figure 4]. This reflects that degeneration progresses from 4–6 M to 9–11 M. The b-wave of all retinal disease mice at 9–11 M became essentially nonrecordable.

TTPs for control, *Bbs1*$^{M390R/M390R}$, *Bbs10*$^{-/-}$, and *Rs1*-KO mice were plotted against their respective ERG SCR b-wave

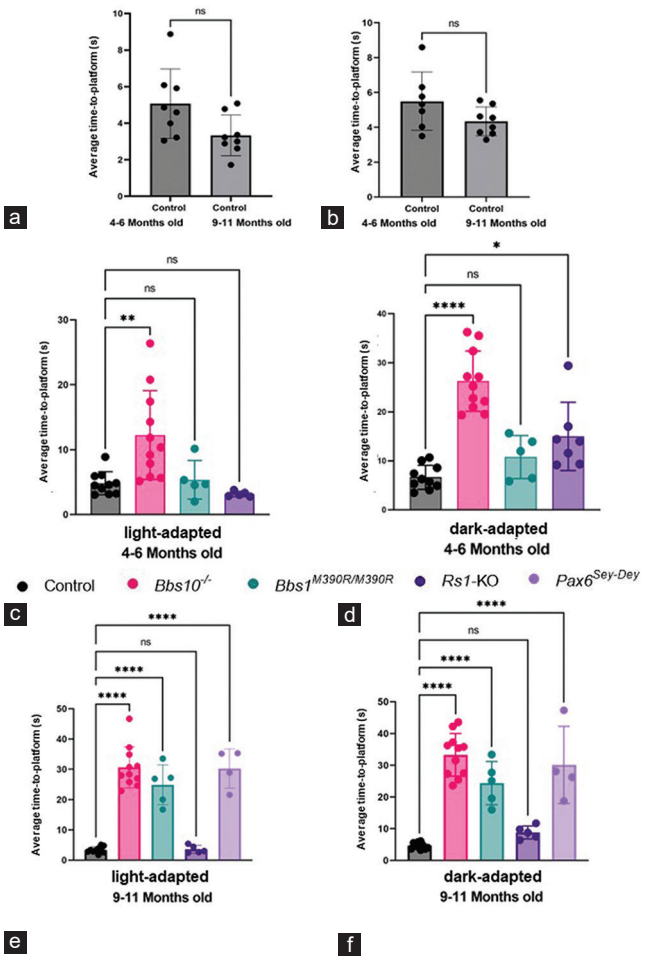

Figure 3: Three different mouse models of retinal dystrophy compared to controls in the visually guided swim assay. (a and b) Comparison of the control group in light-adapted (LA) and dark-adapted (DA) conditions. No significant difference is shown between the control group at both lighting conditions. (c and d) Comparison of Bardet–Biedl syndrome *(Bbs1*$^{M390R/M390R}$*)*, *Bbs10*$^{-/-}$, and *Rs1-KO* mouse models in LA and DA conditions at 4–6 M time point. (e and f) Comparison of *Bbs1*$^{M390R/M390R}$, *Bbs10*$^{-/-}$, *Rs1-KO*, and eyeless *Pax6*$^{Sey\text{-}Dey}$ mouse models in LA and DA conditions at 9–11 M time point. *BBS1*$^{M390R/M390R}$ data were reported previously.[10] Control = Wild type or heterozygous; s = seconds. * = $P < 0.01$, ** = $P < 0.001$, **** = $P < 0.0001$. ns = not significant. BBS: Bardet–Biedl syndrome

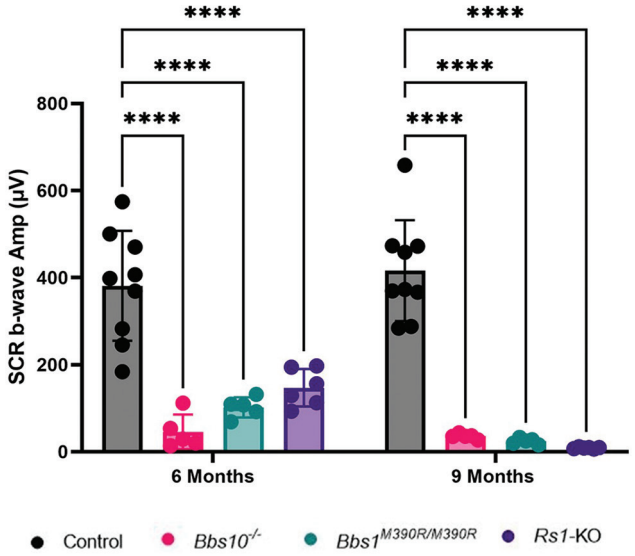

Figure 4: Electroretinogram (ERG) amplitude comparison of all mouse models versus control. ERG amplitudes of Bardet–Biedl syndrome *(Bbs1*$^{M390R/M390R}$*)*, *Bbs10*$^{-/-}$, and *Rs1-KO* mouse models compared to controls at both ages (4–6 M and 9–11 M) in the dark-adapted standard combined response ERG test. Significant difference is shown between all mutant groups compared to controls at both time points. Control = Wild type or heterozygous; s = seconds. **** = $P < 0.0001$. Amp = Amplitude. μV = Microvolt. BBS: Bardet–Biedl syndrome, SCR: Standard combined response

amplitudes at both time points [Figure 5a]. The relationship between ERG b-wave amplitudes and TTP was determined using RStudio [Figure 5a]. As expected, mice with normal vision have higher ERG amplitudes. However, when vision is low, for example, in those mice with retinal disease, the relationship between ERG and vision is not the same. In the "low-vision" zone occupied by all of the retinal disease models, differences in vision detected by longer TTP are not reflected in meaningful differences in ERG recordings. The difference in ERG amplitudes per 5 s difference in TTP is graphed in Figure 5b, showing that when retinal degenerative mice exhibit longer TTP, their ERG are insensitive to these changes. The relationship between ERG and vision is not linear.

We used the VGSA to determine changes in LA visual function in *Bbs10*$^{-/-}$ mice as they aged and compared their LA TTP to the amplitudes of their cone-specific ERG recordings. *Bbs10*$^{-/-}$mice have essentially nonrecordable cone electrical function from a young age.[10,37] Analysis of 5 Hz flicker ERG amplitudes, a measure of cone response, in this model revealed that the 5 Hz flicker amplitudes were essentially nonrecordable at both 4-6 M and 9–11 M (*Bbs10*$^{-/-}$: $r^2 = 0.5003$, $P = 0.086$, simple linear regression) [Figure 5c]. However, this does not mean that their functional vision in the light remains constant over time. At 4–6 M, the *Bbs10*$^{-/-}$ mice exhibited shorter average TTP values compared to their 9–11 M TTP that became longer (4–6 M: 12.24 ± 6.86 s; 9–11 M: 30.66 ± 6.81 s, $P = 0.0004$, simple linear regression) [Figure 5d]. The VGSA captured the gradual loss of LA vision during the disease course of *Bbs10*$^{-/-}$ mice that was not reflected in changes in their cone-specific ERG recordings.

Discussion

The main purpose of this study was the identification of an appropriate endpoint for evaluating therapeutic efficacy in preclinical trials in mouse models of retinal degeneration that would be comparable to the MLMT endpoints elected for human clinical trials of different retinal dystrophies. The direct measurement of functional vision in mice poses practical challenges. For example, the substantial size disparity between the eyes and visual pathways of mice, in comparison to cats or primates, presents considerable obstacles when attempting

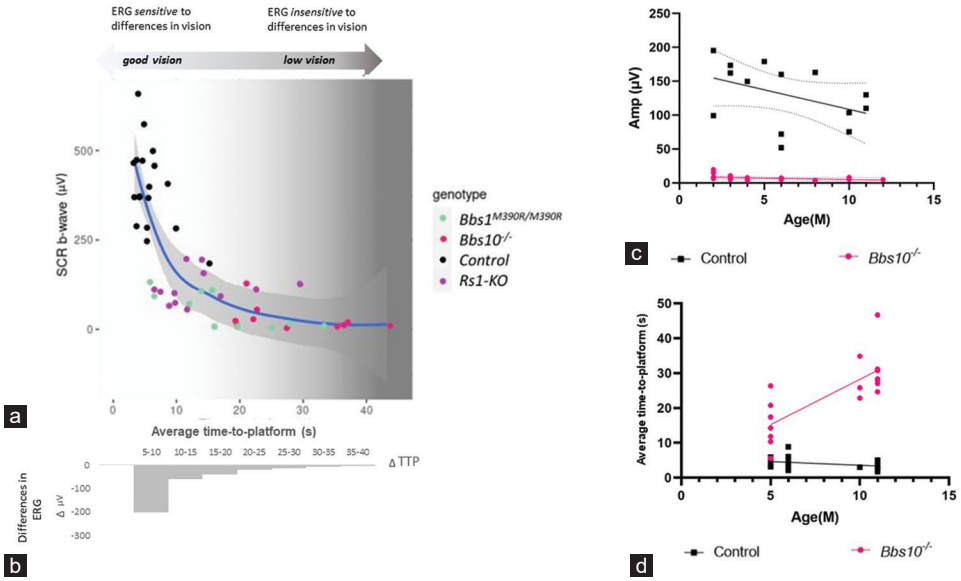

Figure 5: The relationship between electroretinogram (ERG) and functional vision. (a) The standard combined response b-wave amplitudes of control, Bardet–Biedl syndrome *(Bbs1*$^{M390R/M390R}$*), Bbs10*$^{-/-}$, and *Rs1-KO* mice at the age of 4–6 M and 9–11 M are depicted against their respective time-to-platform (TTP) in dark-adapted conditions. (b) The difference in ERG b-wave amplitudes in plot (a), above, per 5-second window[shown in gray blocks in (b)] in TTP is illustrated. In the "low-vision" zone, ERG becomes insensitive, as evidenced by the absence of notable changes in ERG amplitudes despite the lengthening of TTP. (c) Comparison of *Bbs10*$^{-/-}$ and controls 5 Hz ERG amplitudes in the light-adapted (LA) condition showing constant amplitudes over time for both groups. (d) Comparison of *Bbs10*$^{-/-}$ and controls TTP in the LA condition over time showing longer TTP for *Bbs10*$^{-/-}$ as they age and constant TTP in controls. s = seconds. M = months. Amp = Amplitude. μV = Microvolt. BBS: Bardet–Biedl syndrome, SCR: Standard combined response

targeted recordings.[38,39] ERG has been commonly used as a surrogate for vision in mice. However, ERG is not directly correlated with visual function in mice or men. The prevalence of using mouse models to understand disease progression and design therapeutic intervention necessitates the need for a quantitative and reproducible assay for vision in mice. In this current study, we validated such an assay for measuring vision in mice – the VGSA. In addition, using this vision assay, we explored the relationship between ERG amplitudes and TTP.

To validate the VGSA, we first established the range of values in light and dark conditions for mice possessing normal vision and for mice possessing no vision at two different time points, 4–6 and 9–11 months of age. We found that control mice possess stable vision over their lives, consistently taking 3–5 s to locate the platform, while TTP of eyeless *Pax6*$^{Sey\text{-}Dey}$ averaged 7 times longer. These validation tests established the range of expected times for mice with normal vision versus for mice with no vision at all. This evidence shows that eyesight was the primary sense used to find the platform.

To determine whether VGSA can be used to evaluate vision loss in mouse models of heritable retinal disorders, we analyzed the functional vision for three different mouse models exhibiting retinal disease. Mice with BBS, a progressive retinal degeneration, showed significant worsening of TTP as they aged. At the beginning of the assay, when *Bbs1*$^{M390R/M390R}$ and *Rs1*-KO mice were aged 4–6 M, their TTP in bright light closely matched the time of controls. This indicates that functional vision in bright light remained relatively intact. However, a difference from controls appeared in their DA TTP, indicating that there might be some impairment or alteration in their visual capabilities under dark conditions. BBS mice at 9–11 M had TTP that were similar to eyeless (*Pax6*$^{Sey\text{-}Dey}$) mice, indicating that functional vision had deteriorated during disease progression and little or no vision remained. Meanwhile, control mice showed no change in TTP with age. Of interest, in *Rs1*-KO mice, a model of XLRS, which is primarily a maculopathy in humans and relatively stable over many years, the TTP was significantly different from controls only in the dark at the youngest age. As the *Rs1*-KO mice aged, their TTP actually improved, though they still had a higher TTP average compared to controls. At all ages, ERG SCR b-wave was lower for *Rs1*-KO than controls. This suggests that for some retinal diseases (e.g., XLRS), mice like humans may learn to use their defective vision better over time, and ERG does not correlate with functional vision.

We investigated whether the visual function in mice correlates with ERG amplitudes. When we compared the TTP of mice against ERG amplitudes, we observed a nonlinear relationship between ERG values and TTP. ERG amplitudes experience an exponential decrease for the lengthening of TTP. In other words, among the mice with low vision, those with worse vision do not necessarily possess lower ERG amplitudes than those with somewhat better vision. In this range, the ERG test ceased to be a useful approximation of vision. For example, the VGSA detected worsening of LA cone vision *Bbs10*$^{-/-}$ over time, whereas the 5 Hz flicker cone ERG amplitudes were low and did not change over time. This is likely because the ERG is a mass retinal response and there are

far more rods than cones in the mouse retina.[40] In a hypothetical scenario, if there were to be a 50% reduction in rod numbers, it could potentially lead to a noticeable decrease in ERG amplitude. Similarly, if there were a 50% reduction in cone numbers, it is conceivable that the resulting electrical output might be too low to be detectable using our current technology. In addition, the LA VGSA may require a lower number of functional cones to facilitate useful vision compared to the number of functional rods needed in DA conditions. ERG is an important objective measurement of the first part of the visual system, and loss of ERG is an early sign of photoreceptor dysfunction or degeneration as is seen in many inherited retinal degenerations.[10,32] Because it is a mass response, eyes with functional, usable vision in both humans and animals may have a nonrecordable ERG. Vision is a psychophysical function that begins with a photochemical reaction to light but must be propagated to the visual cortex and interpreted by the brain to result in functional vision. For example, in humans with retinitis pigmentosa, the overall electrical response of the retina as measured by ERG may not be detectable. However, the central part of the retina, which mediates central vision, often retains functioning cells, allowing for relatively good visual function. While ERG is commonly used as an endpoint to evaluate the efficacy of potential treatments in preclinical trials, relying solely on ERG measurements may not capture the full extent of therapeutic effects in certain cases.

Conclusion

The VGSA was employed as a means of quantitatively assessing vision under varying levels of illumination, making it analogous to the MLMT which evaluates the capacity to maneuver through a course measuring 5 feet by 10 feet at different light levels. Utilizing the VGSA in mouse preclinical treatment trials for human retinal disease will avoid missing a potentially effective treatment that results in functional vision improvement without a change in ERG, bridging the gap between preclinical research and clinical trials.

Acknowledgment

We thank Val Sheffield, M.D., Ph.D. for *Bbs10*$^{-/-}$ mouse model gift and Paul Sieving, M.D., Ph.D. for *Rs1*-KO mouse model gift.

Financial support and sponsorship

Nil.

Conflicts of interest

There are no conflicts of interest.

References

1. Lai CM, Yu MJ, Brankov M, Barnett NL, Zhou X, Redmond TM, *et al.* Recombinant adeno-associated virus type 2-mediated gene delivery into the Rpe65(-/-) knockout mouse eye results in limited rescue. Genet Vaccines Ther 2004;2:3.
2. Bennicelli J, Wright JF, Komaromy A, Jacobs JB, Hauck B, Zelenaia O, *et al.* Reversal of blindness in animal models of leber congenital amaurosis using optimized AAV2-mediated gene transfer. Mol Ther 2008;16:458-65.
3. Duncan JL, LaVail MM, Yasumura D, Matthes MT, Yang H, Trautmann N, *et al.* An RCS-like retinal dystrophy phenotype in mer knockout mice. Invest Ophthalmol Vis Sci 2003;44:826-38.
4. Phillips MJ, Webb-Wood S, Faulkner AE, Jabbar SB, Biousse V, Newman NJ, *et al.* Retinal function and structure in Ant1-deficient mice. Invest Ophthalmol Vis Sci 2010;51:6744-52.
5. Vollrath D, Yasumura D, Benchorin G, Matthes MT, Feng W, Nguyen NM, *et al.* Tyro3 modulates Mertk-associated retinal degeneration. PLoS Genet 2015;11:e1005723.
6. An GJ, Asayama N, Humayun MS, Weiland J, Cao J, Kim SY, *et al.* Ganglion cell responses to retinal light stimulation in the absence of photoreceptor outer segments from retinal degenerate rodents. Curr Eye Res 2002;24:26-32.
7. Karpe G. Clinical electroretinography. Trans Ophthalmol Soc (UK) 1949;69:237-47.
8. Robson AG, Frishman LJ, Grigg J, Hamilton R, Jeffrey BG, Kondo M, *et al.* ISCEV standard for full-field clinical electroretinography (2022 update). Doc Ophthalmol 2022;144:165-77.
9. Bok D. Gene therapy of retinal dystrophies: Achievements, challenges and prospects. Novartis Found Symp 2004;255:4-12.
10. Mayer SK, Thomas J, Helms M, Kothapalli A, Cherascu I, Salesevic A, *et al*. Progressive retinal degeneration of rods and cones in a Bardet Biedl syndrome type 10 mouse model. Dis Model Mech 2022;15:5-7.
11. Russell S, Bennett J, Wellman JA, Chung DC, Yu ZF, Tillman A, *et al.* Efficacy and safety of voretigene neparvovec (AAV2-hRPE65v2) in patients with RPE65-mediated inherited retinal dystrophy: A randomised, controlled, open-label, phase 3 trial. Lancet 2017;390:849-60.
12. Chung DC, McCague S, Yu ZF, Thill S, DiStefano-Pappas J, Bennett J, *et al.* Novel mobility test to assess functional vision in patients with inherited retinal dystrophies. Clin Exp Ophthalmol 2018;46:247-59.
13. Ahmed F, Rajendran Nair DS, Thomas BB. A new optokinetic testing method to measure rat vision. J Vis Exp 2022 ;185:1-7.
14. Shi C, Yuan X, Chang K, Cho KS, Xie XS, Chen DF, *et al.* Optimization of optomotor response-based visual function assessment in mice. Sci Rep 2018;8:9708.
15. Pang JJ, Chang B, Kumar A, Nusinowitz S, Noorwez SM, Li J, *et al.* Gene therapy restores vision-dependent behavior as well as retinal structure and function in a mouse model of RPE65 leber congenital amaurosis. Mol Ther 2006;13:565-72.
16. Pang JJ, Boye SL, Kumar A, Dinculescu A, Deng W, Li J, *et al.* AAV-mediated gene therapy for retinal degeneration in the rd10 mouse containing a recessive PDEbeta mutation. Invest Ophthalmol Vis Sci 2008;49:4278-83.
17. Prusky GT, West PW, Douglas RM. Behavioral assessment of visual acuity in mice and rats. Vision Res 2000;40:2201-9.
18. Sarria I, Pahlberg J, Cao Y, Kolesnikov AV, Kefalov VJ, Sampath AP, *et al.* Sensitivity and kinetics of signal transmission at the first visual synapse differentially impact visually-guided behavior. Elife 2015;4:e06358.
19. Laird JG, Gardner SH, Kopel AJ, Kerov V, Lee A, Baker SA. Rescue of rod synapses by induction of Cav Alpha 1F in the mature Cav1.4 knock-out mouse retina. Invest Ophthalmol Vis Sci 2019;60:3150-61.
20. Weihbrecht K, Goar WA, Pak T, Garrison JE, DeLuca AP, Stone EM, *et al*. Keeping an eye on Bardet Biedl syndrome: A comprehensive review of the role of Bardet Biedl syndrome genes in the eye. Med Res Arch 2017;5:1-9.
21. Mardy AH, Hodoglugil U, Yip T, Slavotinek AM. Third case of Bardet-Biedl syndrome caused by a biallelic variant predicted to affect splicing of IFT74. Clin Genet 2021;100:93-9.
22. Zhou Z, Qiu H, Castro-Araya RF, Takei R, Nakayama K, Katoh Y. Impaired cooperation between IFT74/BBS22-IFT81 and IFT25-IFT27/BBS19 causes Bardet-Biedl syndrome. Hum Mol Genet 2022;31:1681-93.
23. Vijayasarathy C, Zeng Y, Brooks MJ, Fariss RN, Sieving PA. Genetic rescue of X-linked retinoschisis mouse (Rs1(-/y)) retina induces quiescence of the retinal microglial inflammatory state following AAV8-RS1 gene transfer and identifies gene networks underlying retinal recovery. Hum Gene Ther 2021;32:667-81.
24. Hill RE, Favor J, Hogan BL, Ton CC, Saunders GF, Hanson IM, *et al.* Mouse small eye results from mutations in a paired-like

homeobox-containing gene. Nature 1992;355:750.
25. Theiler K, Varnum DS, Stevens LC. Development of Dickie's small eye, a mutation in the house mouse. Anat Embryol (Berl) 1978;155:81-6.
26. Davis RE, Swiderski RE, Rahmouni K, Nishimura DY, Mullins RF, Agassandian K, *et al*. A knockin mouse model of the Bardet-Biedl syndrome 1 M390R mutation has cilia defects, ventriculomegaly, retinopathy, and obesity. Proc Natl Acad Sci U S A 2007;104:19422-7.
27. Cring MR, Meyer KJ, Searby CC, Hedberg-Buenz A, Cave M, Anderson MG, *et al.* Ectopic expression of BBS1 rescues male infertility, but not retinal degeneration, in a BBS1 mouse model. Gene Ther 2022;29:227-35.
28. Zeng Y, Takada Y, Kjellstrom S, Hiriyanna K, Tanikawa A, Wawrousek E, *et al.* RS-1 gene delivery to an adult Rs1h knockout mouse model restores ERG b-wave with reversal of the electronegative waveform of X-linked retinoschisis. Invest Ophthalmol Vis Sci 2004;45:3279-85.
29. Bush RA, Zeng Y, Colosi P, Kjellstrom S, Hiriyanna S, Vijayasarathy C, *et al.* Preclinical dose-escalation study of intravitreal AAV-RS1 gene therapy in a mouse model of X-linked retinoschisis: Dose-dependent expression and improved retinal structure and function. Hum Gene Ther 2016;27:376-89.
30. Weber BH, Schrewe H, Molday LL, Gehrig A, White KL, Seeliger MW, *et al.* Inactivation of the murine X-linked juvenile retinoschisis gene, Rs1h, suggests a role of retinoschisin in retinal cell layer organization and synaptic structure. Proc Natl Acad Sci U S A 2002;99:6222-7.
31. Morris R. Developments of a water-maze procedure for studying spatial learning in the rat. J Neurosci Methods 1984;11:47-60.
32. Hsu Y, Bhattarai S, Thompson JM, Mahoney A, Thomas J, Mayer SK, *et al.* Subretinal gene therapy delays vision loss in a Bardet-Biedl syndrome type 10 mouse model. Mol Ther Nucleic Acids 2023;31:164-81.
33. Nunez J. Morris water maze experiment. J Vis Exp 2008;19:897.
34. Tucker LB, Velosky AG, McCabe JT. Applications of the Morris water maze in translational traumatic brain injury research. Neurosci Biobehav Rev 2018;88:187-200.
35. McCulloch DL, Marmor MF, Brigell MG, Hamilton R, Holder GE, Tzekov R, *et al.* ISCEV standard for full-field clinical electroretinography (2015 update). Doc Ophthalmol 2015;130:1-12.
36. Grudzinska Pechhacker MK, Jacobson SG, Drack AV, Scipio MD, Strubbe I, Pfeifer W, *et al.* Comparative natural history of visual function from patients with biallelic variants in BBS1 and BBS10. Invest Ophthalmol Vis Sci 2021;62:26.
37. Fu Y, Yau KW. Phototransduction in mouse rods and cones. Pflugers Arch 2007;454:805-19.
38. Remtulla S, Hallett PE. A schematic eye for the mouse, and comparisons with the rat. Vision Res 1985;25:21-31.
39. Huberman AD, Niell CM. What can mice tell us about how vision works? Trends Neurosci 2011;34:464-73.
40. Beales PL, Elcioglu N, Woolf AS, Parker D, Flinter FA. New criteria for improved diagnosis of Bardet-Biedl syndrome: Results of a population survey. J Med Genet 1999;36:437-46.